ANALYSIS OF TWO-DIMENSIONAL RIVERBED VARIATION IN CHANNELS WITH STONY BEDS

Kengo OSADA[1], and Shoji FUKUOKA[2]
1. Research and Development Initiative, Chuo University, Tokyo, ON, Japan (osada@tamacc.chuo-u.ac.jp)
2. Research and Development Initiative, Chuo University, Tokyo, ON, Japan (sfuku@tamacc.chuo-u.ac.jp)

ABSTRACT

In a stony-bed river with wide grain-size distribution, boulders that would not move during a flood act as strong fluid-resistance element. In addition, sand and gravel often remain in the bed irregularities formed by large stones. A stony-bed river will remain in a static equilibrium condition when the river bed surface grain size distributions corresponding to tractive force of the flow are reached. However, conventional riverbed variation analysis does not account for these essential mechanisms in stony-bed rivers. Therefore, we had developed a one-dimensional riverbed variation analysis method by considering the mechanism of riverbed variation in stony bed rivers. This method is generally capable of explaining water surface profile, quantitative bed variation, and bed material size distribution in stony-bed rivers. In this study, we developed the method of two-dimensional riverbed variation analysis by considering the mechanism of riverbed variation and bank erosion in stony bed rivers. We verified the applicability of the model with the field experimental results which was conducted in the meandering channel in the Jyoganji River.

1. INTRODUCTION

In stony bed rivers with wide grain size distribution, flow resistance is determined by the drag force acting on large stones. In addition, sand and gravel often remain in the bed irregularities formed by large stones. A stony-bed river will remain in a static condition (Fukuoka et al., 2008). However, it is difficult to simulate riverbed variations in stony-bed rivers by the conventional river bed variation analysis methods, which does not account for these essential mechanisms by large stones in stony-bed rivers. To improve channel planning in stony-bed rivers, a accurate technique for riverbed variation is required (Fukuoka, 2008).

The authors have conducted large scale field experiments in the Jyoganji River to elucidate the mechanism of bed variation in stony-bed rivers with wide grain size distributions (Fukuoka and Abe, 2007). We had developed the new method of one-dimensional riverbed variation analysis based on the following important mechanism of bed variation in stony-bed rivers (Osada and Fukuoka, 2008). First, sediment transport of small size materials depend on large stones. The amount of sediment transport of the small size materials is difficult to estimate from equilibrium sediment transport formula with the critical tractive force. The sediment transport model is composed of pick-up rate from the riverbed and deposit rate to the riverbed. Second, large voids are formed by exposed large stones on the riverbed surface. The large voids on the riverbed surface are important to analysis of bed variation in the stony bed rivers. To take account for the large voids, we calculated the heights of each size group on the riverbed surface. Third, to consider the form resistance of large stones, we developed the resistance formula using d_{90} in the bed surface. It was demonstrated that water surface profile, bed variation and grain size distribution in straight channels with stony bed were estimated by the one-dimensional analysis.

In this study, we develop a numerical method of two-dimensional bed variation by considering mechanism of sediment transport and bank erosion in stony bed rivers. It is important for the two-dimensional analysis method to estimate bank erosion and sediment transport in the transverse direction. In general, bank erosion rate in sand and gravel bed rivers is calculated with the Hasegawa's method (Hasegawa, 1981). In this method, river bank is collapsed when the side slope of the bank exceeds the angle of repose. In the stony bed rivers, cobbles and boulders deposits into the riverbed near the bank due to the bank erosion, and the riverbed become stable condition. Hasegawa's method by using angle of repose estimates the bank erosion to be large. Therefore, this method is difficult to apply to bank erosion in stony-bed rivers. We propose pick-up rate formula to account for the bank erosion in stony bed rivers. We verified the applicability of the model by the field experimental results conducted by the meandering channel in the Jyoganji River (Fukuoka and Osada, 2009).

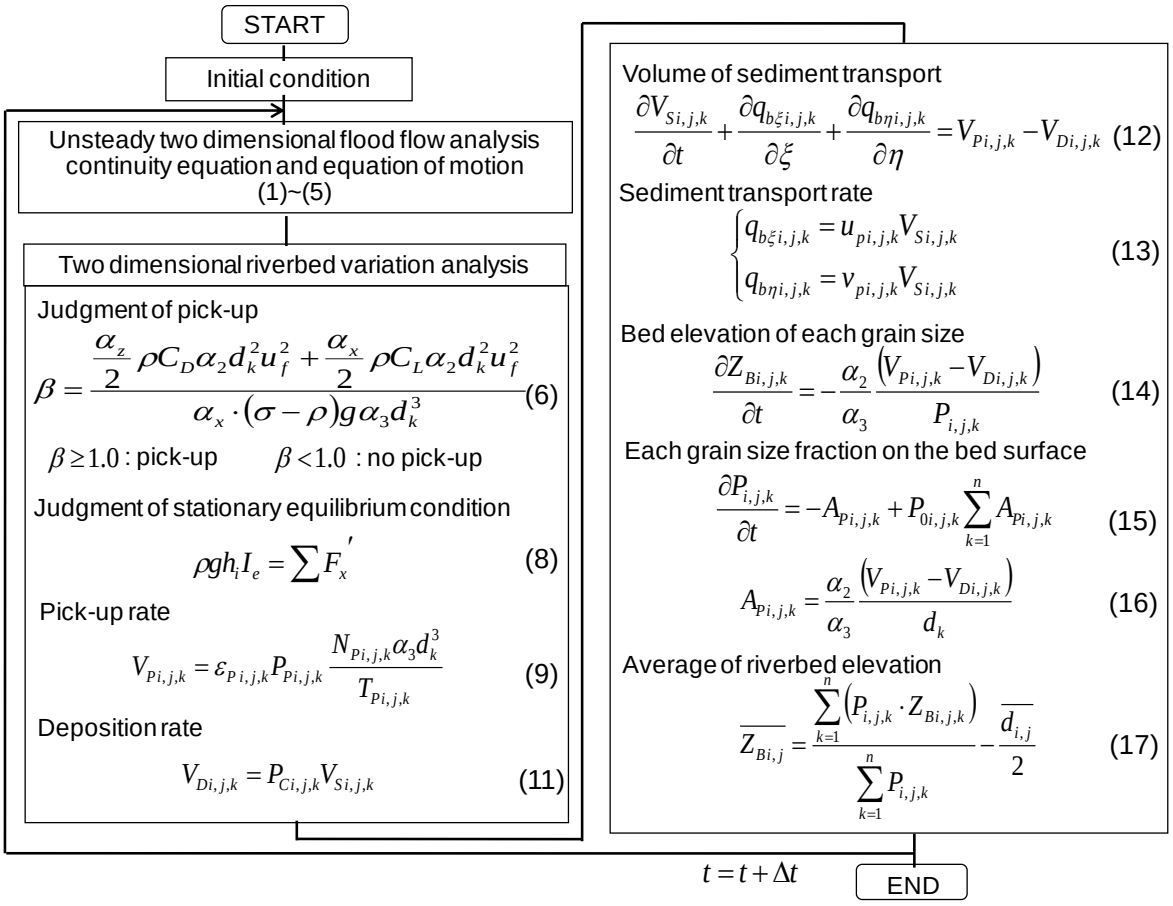

Figure 1 Procedure of the two-dimensional riverbed variation analysis

2. TWO-DIMENSIONAL RIVERBED VARIATION ANALYSIS FOR STONY-BED RIVERS

Figure 1 shows the procedure of the two-dimensional riverbed variation analysis. In this method, we use combination of the unsteady two-dimensional flow analysis and the two-dimensional bed variation analysis. The flood flow is calculated by equations (1)~(3).

$$\frac{\partial}{\partial t}\left(\frac{h}{J}\right) + \frac{\partial}{\partial \xi}\left(\frac{q^{\xi}}{J}\right) + \frac{\partial}{\partial \eta}\left(\frac{q^{\eta}}{J}\right) = 0 \quad (1)$$

$$\frac{\partial}{\partial t}\left(\frac{q^{\xi}}{J}\right)+\frac{\partial}{\partial \xi}\left(\frac{u^{\xi}q^{\xi}}{J}\right)+\frac{\partial}{\partial \eta}\left(\frac{u^{\eta}q^{\xi}}{J}\right)-\frac{q_x}{J}\left(u^{\xi}\frac{\partial \xi_x}{\partial \xi}+u^{\eta}\frac{\partial \xi_x}{\partial \eta}\right)-\frac{q_y}{J}\left(u^{\xi}\frac{\partial \xi_y}{\partial \xi}+u^{\eta}\frac{\partial \xi_y}{\partial \eta}\right)$$
$$=-gh\left(\frac{\xi_x^2+\xi_y^2}{J}\frac{\partial H}{\partial \xi}+\frac{\xi_x\eta_x+\xi_y\eta_y}{J}\frac{\partial H}{\partial \eta}\right)-\frac{F_{D90}^{\xi}}{\rho J}+\frac{\xi_x^2}{J}\frac{\partial}{\partial \xi}\left(-\overline{u_x'^2}h\right)+\frac{\xi_x\eta_x}{J}\frac{\partial}{\partial \eta}\left(-\overline{u_x'^2}h\right) \quad (2)$$
$$+\frac{\xi_y^2}{J}\frac{\partial}{\partial \xi}\left(-\overline{u_y'^2}h\right)+\frac{\xi_y\eta_y}{J}\frac{\partial}{\partial \eta}\left(-\overline{u_y'^2}h\right)+\frac{\xi_x\eta_y+\xi_y\eta_x}{J}\frac{\partial}{\partial \eta}\left(-\overline{u_x'u_y'}h\right)+\frac{2\xi_x\xi_y}{J}\frac{\partial}{\partial \xi}\left(-\overline{u_x'u_y'}h\right)+S_{\xi}$$

$$\frac{\partial}{\partial t}\left(\frac{q^{\eta}}{J}\right)+\frac{\partial}{\partial \xi}\left(\frac{u^{\xi}q^{\eta}}{J}\right)+\frac{\partial}{\partial \eta}\left(\frac{u^{\eta}q^{\eta}}{J}\right)-\frac{q_x}{J}\left(u^{\xi}\frac{\partial \eta_x}{\partial \xi}+u^{\eta}\frac{\partial \eta_x}{\partial \eta}\right)-\frac{q_y}{J}\left(u^{\xi}\frac{\partial \eta_y}{\partial \xi}+u^{\eta}\frac{\partial \eta_y}{\partial \eta}\right)$$
$$=-gh\left(\frac{\xi_x\eta_x+\xi_y\eta_y}{J}\frac{\partial H}{\partial \xi}+\frac{\eta_x^2+\eta_y^2}{J}\frac{\partial H}{\partial \eta}\right)-\frac{F_{D90}^{\eta}}{\rho J}+\frac{\eta_x^2}{J}\frac{\partial}{\partial \eta}\left(-\overline{u_x'^2}h\right)+\frac{\xi_x\eta_x}{J}\frac{\partial}{\partial \xi}\left(-\overline{u_x'^2}h\right) \quad (3)$$
$$+\frac{\eta_y^2}{J}\frac{\partial}{\partial \eta}\left(-\overline{u_y'^2}h\right)+\frac{\xi_y\eta_y}{J}\frac{\partial}{\partial \xi}\left(-\overline{u_y'^2}h\right)+\frac{\xi_x\eta_y+\xi_y\eta_x}{J}\frac{\partial}{\partial \xi}\left(-\overline{u_x'u_y'}h\right)+\frac{2\eta_x\eta_y}{J}\frac{\partial}{\partial \eta}\left(-\overline{u_x'u_y'}h\right)+S_{\eta}$$

Where h : water depth, q^{ξ},q^{η}: contravariant components of flow discharge in the ξ and η direction, u^{ξ},u^{η}: contravariant components of velocity in the ξ and η direction, J : Jacobian of transformation, q_x,q_y: flow discharge per unit width in the x and y direction, $-\overline{u_x'^2},-\overline{u_y'^2},-\overline{u_x'^2u_y'^2}$: Reynolds stress tensors, and $F_{D90}^{\xi},F_{D90}^{\eta}$: The bed resistance. These are calculated by equations (4) and (5).

$$\begin{cases} F_{D90}^{\xi}=\xi_x F_x+\xi_y F_y \\ F_{D90}^{\eta}=\eta_x F_x+\eta_y F_y \end{cases} \quad (4)$$

$$\begin{cases} F_x=N_{D90}\dfrac{\varepsilon_{D90}}{2}\rho C_D\alpha_2 d_{90}^2 u_f^2\cdot\dfrac{u_x}{\sqrt{u_x^2+u_y^2}} \\ F_y=N_{D90}\dfrac{\varepsilon_{D90}}{2}\rho C_D\alpha_2 d_{90}^2 u_f^2\cdot\dfrac{u_y}{\sqrt{u_x^2+u_y^2}} \end{cases} \quad (5)$$

Where N_{D90} : the number of d_{90} per unit area, ε_{D90} : the shielding coefficient of d_{90}, α_2,α_3 : 2-D and 3-D shape factors of the particles, C_D: drag coefficient, u_f is the velocity acting on d_{90} which is determined by logarithmic velocity distribution. And, we add the secondary flow term (S_{ξ},S_{η}) proposed by Nagata et al. (1999) into equation of motion(2),(3).

Next, we explain the two dimensional riverbed variation analysis method. Pick-up judgment of each particle is evaluated by the moment balance equation (equation (6)). The concept of pick up judgment is shown in Figure 2. The angle θ_k is calculated with equation (7).

$$\theta_k=90.0-45.0\cdot\exp\left\{\frac{1}{2}\frac{\left(Z_{Bi,j,k}-Z_{d80i,j}\right)}{d_{80i,j}}\right\}-\theta_{Ci,j} \quad (7)$$

Where subscript k : the number of each grain size material, subscript i, j indicates the computational grid number, $Z_{Bi,j,k}$: height of diameter d_k, $Z_{d80i,j}$: height of d_{80}. $\theta_{Ci,j}$: Riverbed and side bank slope of right direction for velocity. This equation represents the relationship between the height of d_{80} and the height of each particle. For instance, when the height of each particle is lower than the height of d_{80}, angle θ_k is greater than 45°. This means that the particle cannot move easily. On the other hand, when the height of each particle is higher than the height of d_{80}, angle θ_k is smaller than 45°. In addition, the effect of the side bank slope is considered by $\theta_{Ci,j}$.

Next we explain the method of determining bed stability. In the calculations, when d_{80} and d_{90} do not move, fluid force act on those particles. In this instance, the pick-up quantities of all particles from the bed become zero.

After the process outlined up to this point, equation (9) is used to determine the pick-up rate. Here, $\varepsilon_{Pi,j,k}$ is a coefficient that accounts for the shielding effect of particles larger than d_k, $P_{Pi,j}$ is the ratio between the fluid field force acting on the bed and the total drag force acting on the particle, and is calculated as follows:

$$P_{Pi,j} = \frac{\rho g h_{i,j} I_e}{\sum_{k=1}^{n}\left(\frac{N_{Pi,j,k}}{2}\rho C_D \alpha_2 d_k^2 u_f^2\right)} \tag{10}$$

T_{Pk} is defined as the time required for a particle to be transported as shown in Figure 2. Figure 3 show the computational grid. Sediment deposition rate V_D, sediment volume V_S and bed height of each particle size Z_{Bk} are calculated at the center of the grid. And, pick-up rate V_P is calculated at center of the side line.

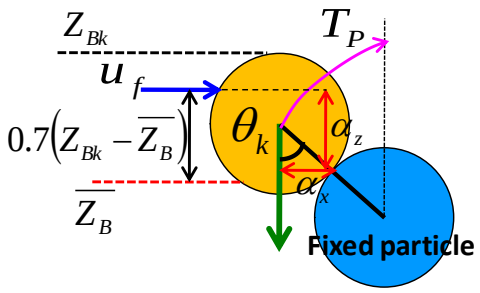

Figure 2 Concept of the pick-up particle

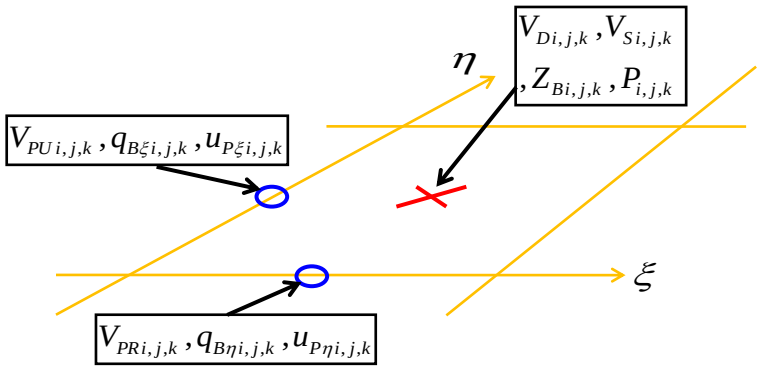

Figure 3 Calculation grid

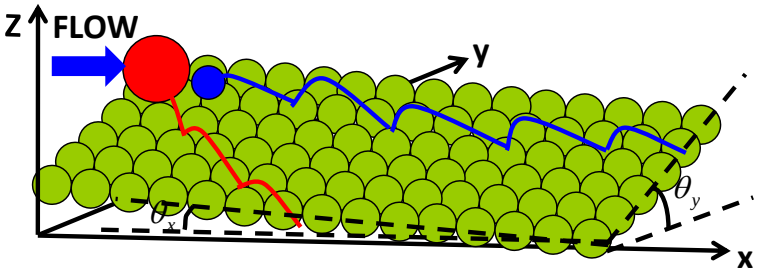

Figure 4 Concept of the saltation analysis

We assume that sediment deposition in stony bed rivers is occurred by collision event between transport particles and riverbed materials. Therefore, sediment deposition rate V_D is calculated by equation (11) using sediment volume V_S and rest ratio P_C that is discussed below. Sediment volume is calculated by equation (12). Sediment transport rate is calculated by equation (13). Here, u_p, v_p are particle velocity. Particle velocity is determined by dividing the calculated time (5 seconds) into the particle's movement distance determined by the saltation time calculations. The author's method includes calculating 5-second saltation using the particle equation of motion, then determining the bed particle collision rate, which is wed to evaluate the rest rate.
The heights of each particle size group are calculated using each size group's pick up quantity from the bed, deposition quantity to the bed, and the bed surface ratio of d_k particles with equation (14). As seen in equations (15) and (16), the surface ratio of areas occupied each particle size group is calculated by each size group's pick up and deposition quantity. Here, $P_{0i,k}$ is the subsurface particle diameter ratio. Average bed height, which is needed to calculate the flow field, is calculated by the equation (17). The first term on the right side of equation (17) is the average particle height in the computational grid, and the second term on the right is radius of the average-diameter particle.

3. APPLICATION TO FIELD EXPERIMENTAL RESULTS IN MEANDERING CHANNEL IN THE JYOGANJI RIVER

3.1 Conditions of Calculations

We apply the bed variation analysis method to the results of field experiments conducted in the Jyoganji River in 2006. Figure 5 is a top view of the meandering channel. The channel contained two meanders, it was dug into a sandbar at the 11.1 km point in the Jyoganji River. The channel was a 120m long, 3m wide and side slope 1:1. Meander 1 contained natural riverbanks, while revetments were built along the outer bank of meander 2. We measured water level by the pressure gauges and level surveying, discharge, bed cross-section, and bed grain size distribution. Table 1 shows the flow discharges of the experiment. Peak discharge of the experiment was 11m^3/s.
The computational grid is made by 2.5m intervals in the downstream-direction and 0.35m intervals in the across-direction. We use observed water level hydrographs at W02 and W21 as the boundary conditions.
Figure 6 shows the grain size distributions using this calculation. The grain size distribution was based on the dimensionless particle size distribution determined by Kuroda and Fukuoka et al. (2005). Seven particle sizes were used in the calculations—350mm, 270mm, 200mm, 120mm, 80mm, 50mm, and 25 mm.

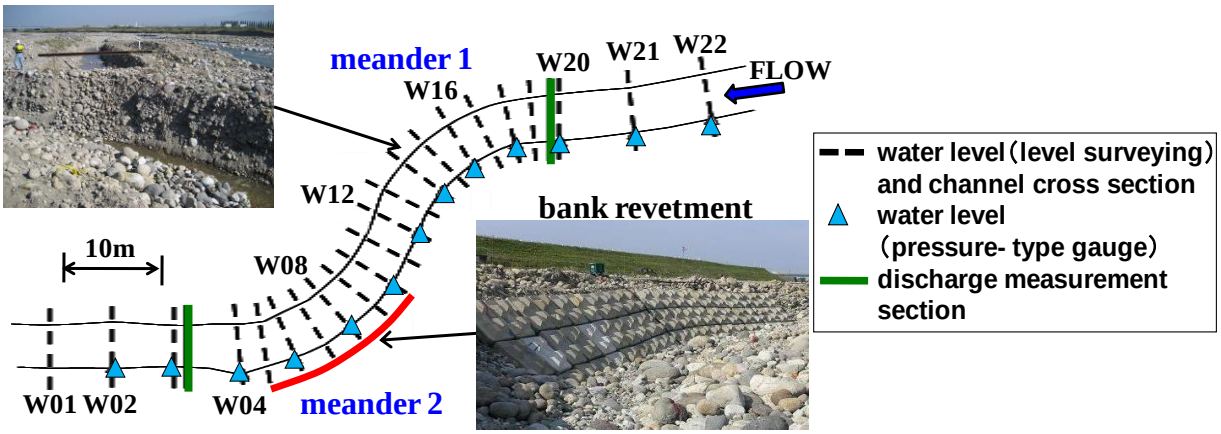

Figure 5　Plan view of the experimental channel

Table 1　Observed discharge

case		S1	S2	S3
upstream	observed time	10:50	11:16	11:35
	discharge(m^3/s)	4.0	6.3	10.9
downstream	observed time	10:50	11:15	11:34
	discharge(m^3/s)	2.8	5.7	10.1

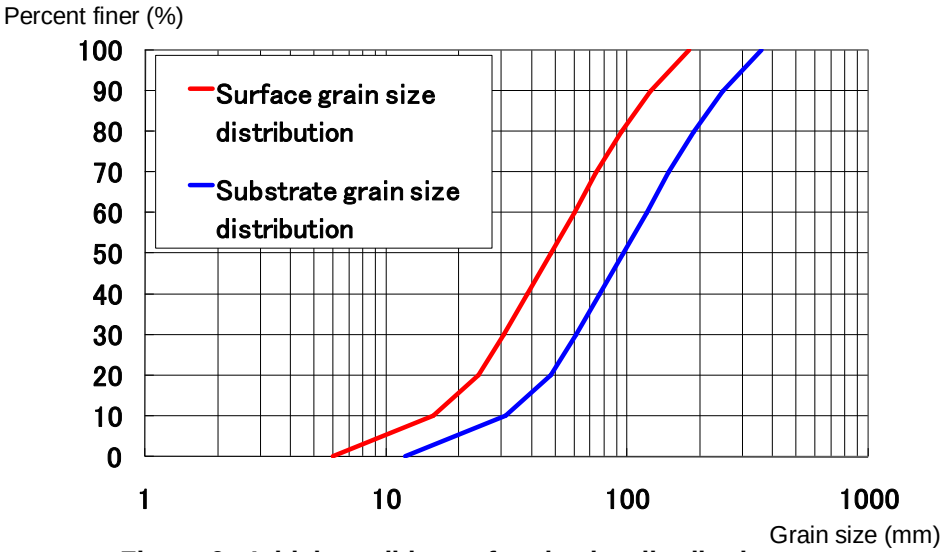

Figure 6　Initial conditions of grain size distribution

3.2 Result of Calculation

Figure 7 and Figure 8 show the calculated and observed temporal change in water level profiles. And, Figure 9(a)~(c) shows the temporal changes in calculated bed variation contour. Looking at the results for water levels (Figure 7, Figure 8), we can see that the calculated results differ about 10cm from the observed water surface profile in the section of meander 1. But, the calculation results almost reproduce the observed water surface profiles. In the Figure 9(b) of the maximum discharge in the hydrograph, bank erosion in the outer bank of the meander 1 and aggradations by sediment deposition in the inner bank of meander 2 become large, comparing with Figure 9(a) of the earlier stage. After the maximum discharge, the bed elevation is almost maintained. Figure 9(d) show the observed bed variation. The calculated result (Figure 9(c)) is agreement with experimental result. However, we have to improve the evaluation method for the amount of bank erosion and sediment deposition in meander 1. Figure 10 shows the bed cross-section profiles. In the W20 located in the straight channel section, calculated bed variation reproduce riverbed aggradations and bank erosion of the experiment. In the W14 where located in meander 1, calculated bed variation cannot explain well for sediment deposition in the inner bank.

Figure 11 shows the comparison between observed and calculated discharge hydrographs. The calculated discharge hydrograph reproduces the observed discharge hydrograph, because calculated water surface profile and bed elevation are good agreement with observed values. Figure 12 shows the transverse distribution of sediment discharge per unit width for each particle size at W19 and W14. In the W19 located in straight channel section, sediment discharges excluding grain size 80mm around center of the channel are lower than. On the other hand, sediment discharges around bank are large than that of the channel center. Around the channel center, stable riverbed is formed by armoring due to bed scour caused by low flow discharge. Around bank, sediment discharge becomes larger than around the channel center due to bank erosion caused by large flow discharge. The data in Figure 12 for the sediment transport of each bed material indicate that 80mm and 120mm particles move actively. The shielding effect of the large size material reduced the sediment discharge of 25mm. Sediment discharge express as following characteristics in the section W14 (Figure 12(b)). Sediment discharge is large around outer bank, whereas it is low around inner bank. Figure 13 show the comparison between observed and calculated grain size d_{80} longitudinal distribution. In the meander section, the calculated d_{80} distribution cannot reproduce the experimental d_{80} distribution. However, as a whole, the calculated results generally agree with the observed results. Figure 14 shows calculated results of d_{80} cross-sectional distribution. Mild slope and armoring near the bank are formed by the supply of cobbles and boulders due to bank erosion. The calculation result reproduces the mild slope and armoring near the bank.

As discussed above, the two-dimensional model is generally capable of explaining water surface profile, bed variation, and bed material size distribution in stony-bed rivers with a wide range of bed material sizes.

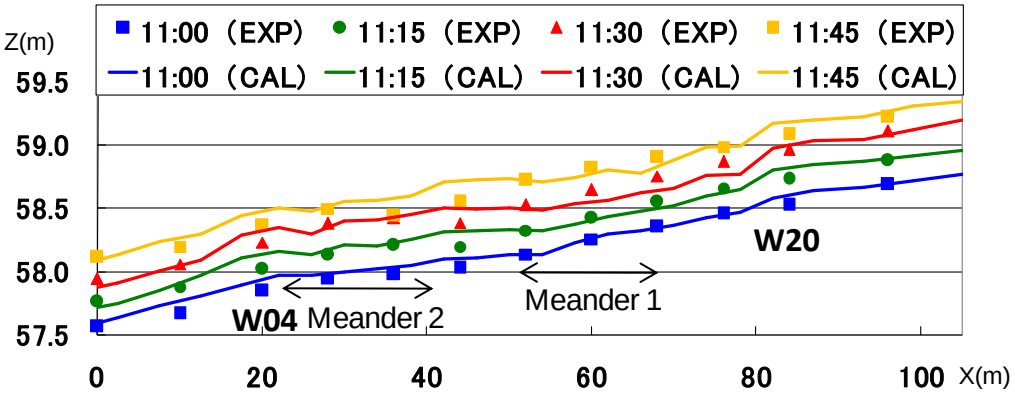

Figure 7 Comparison between observed and calculated water surface profile (Left bank)

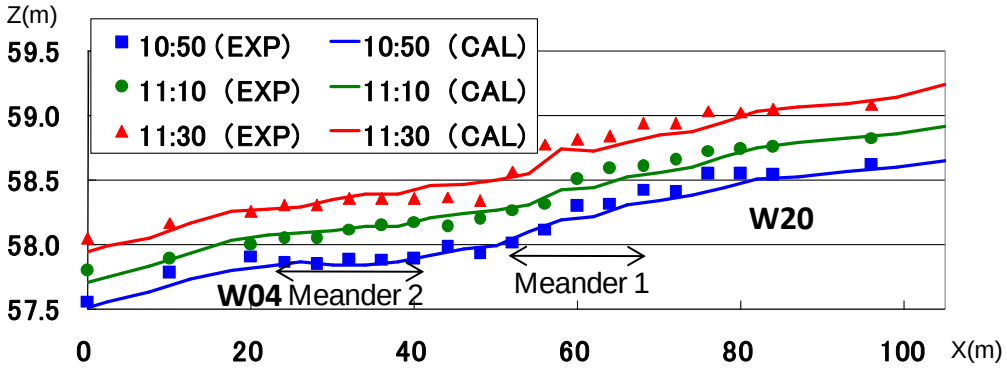

Figure 8 Comparison between observed and calculated water surface profile (Right bank)

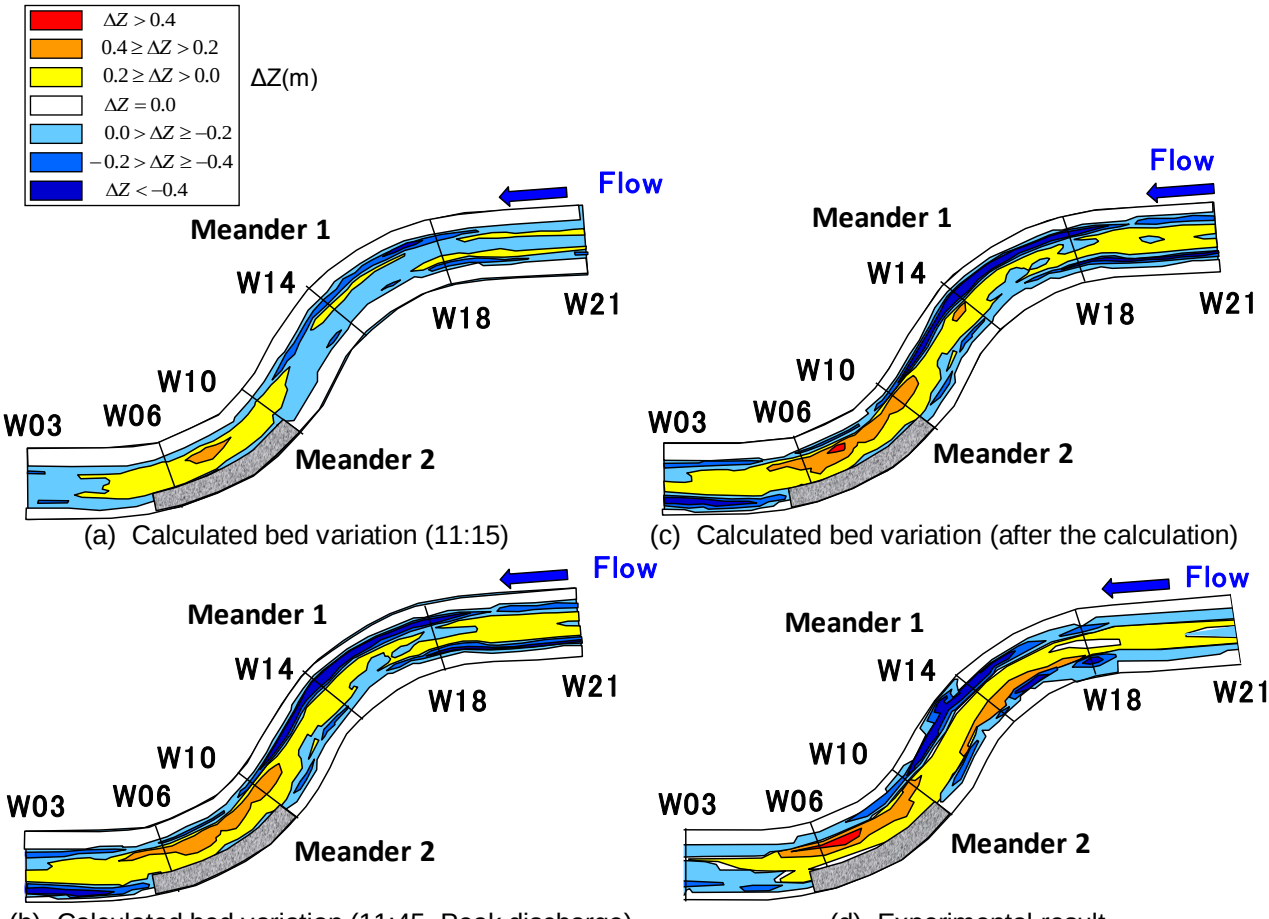

(a) Calculated bed variation (11:15)

(c) Calculated bed variation (after the calculation)

(b) Calculated bed variation (11:45, Peak discharge)

(d) Experimental result

Figure 9 Comparison between observed and calculated bed variation contour

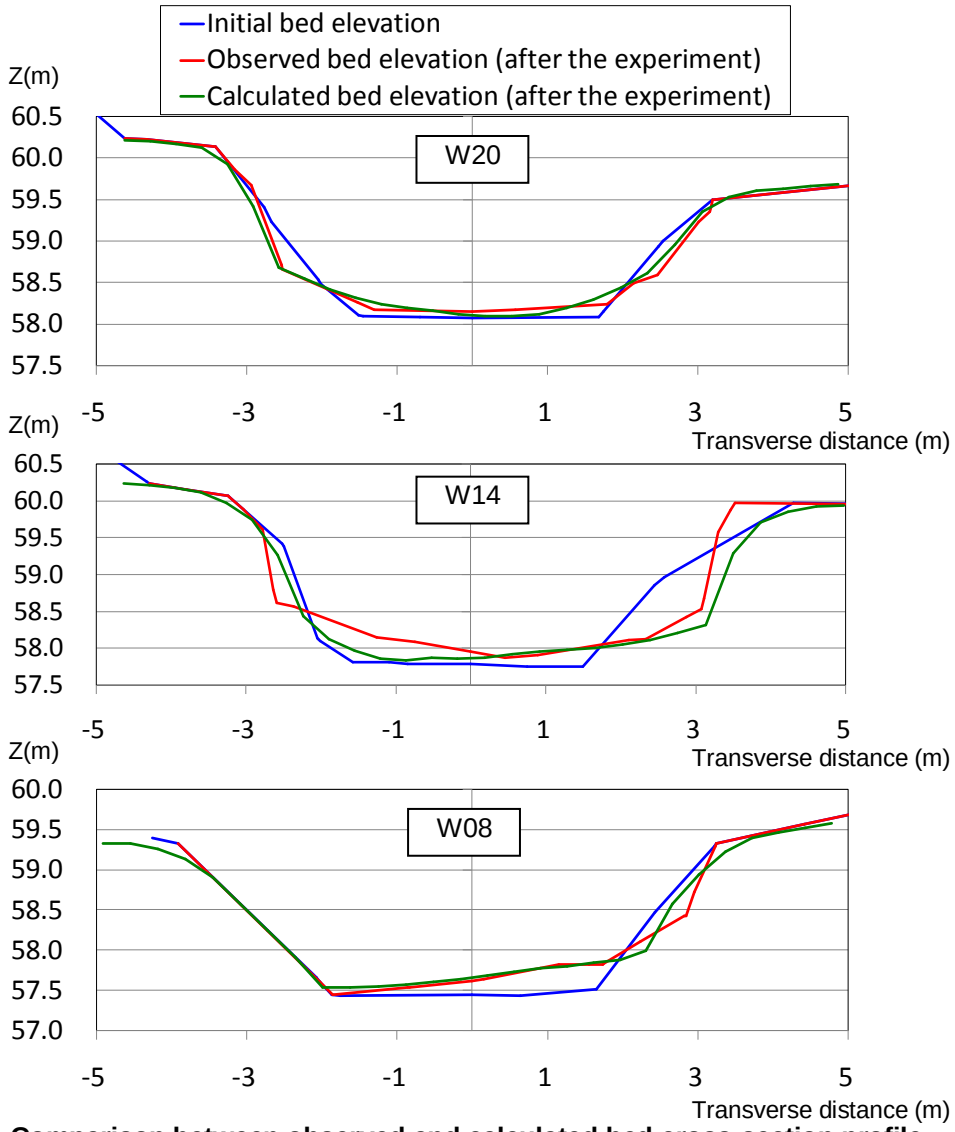

Figure 10 Comparison between observed and calculated bed cross-section profile

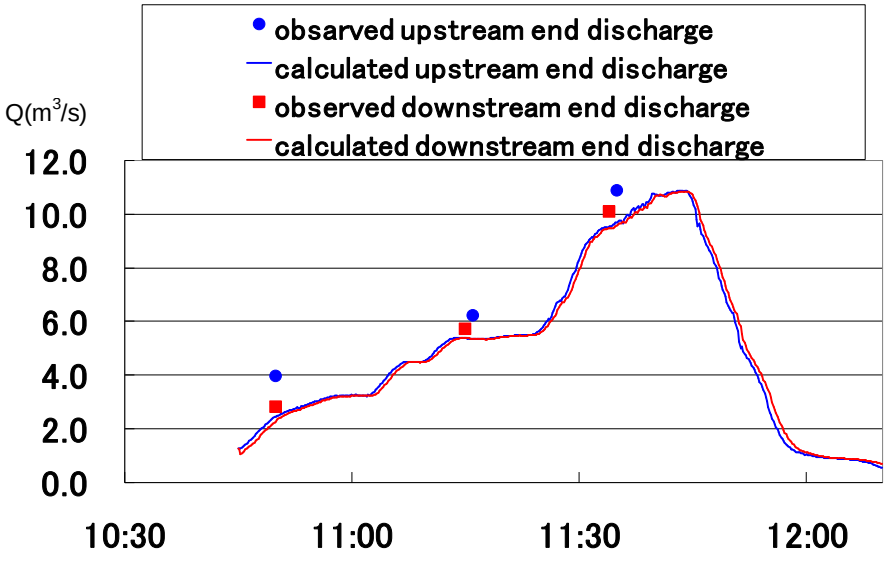

Figure 11 Comparison between observed and calculated discharge hydrographs

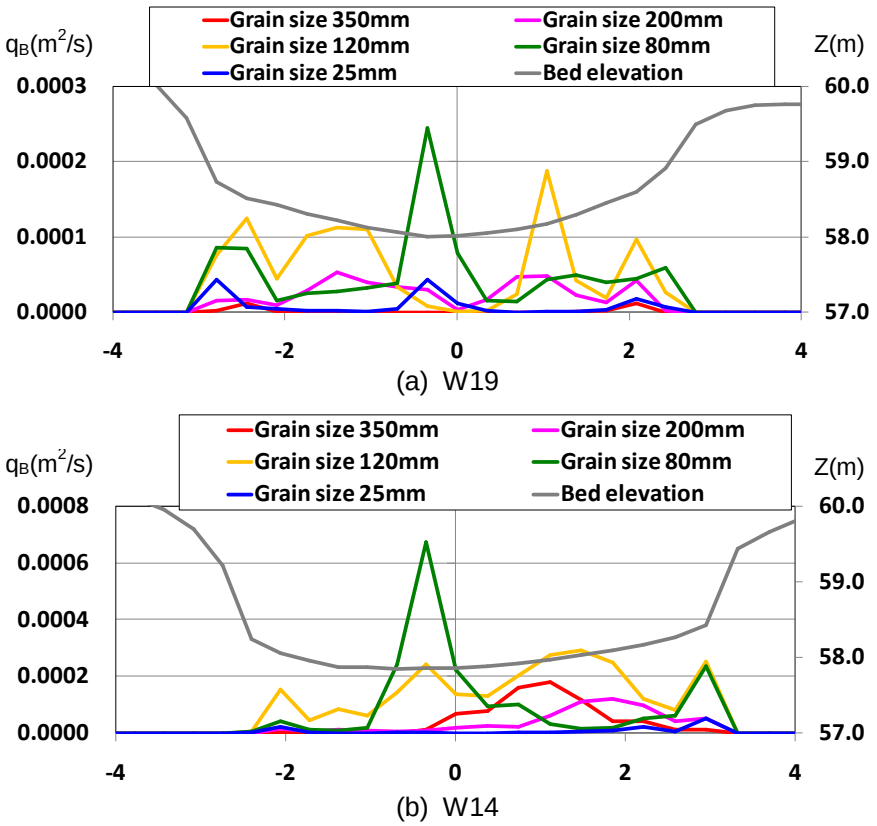

Figure 12 Sediment discharge cross-section profile for each particle size

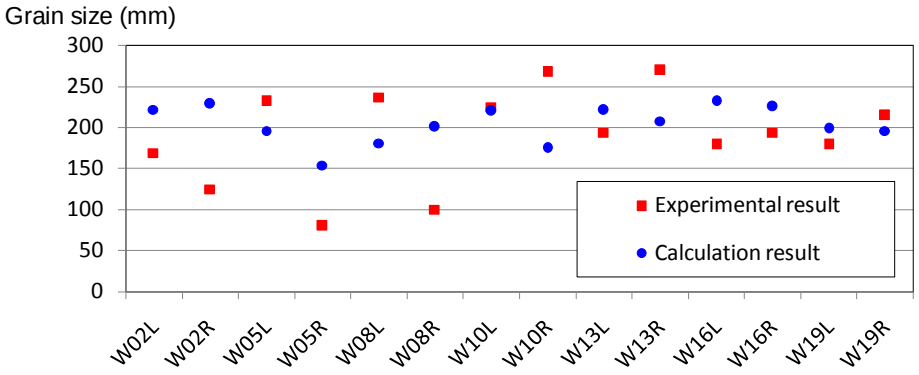

Figure 13 Comparison between observed and calculated grain size d_{80}

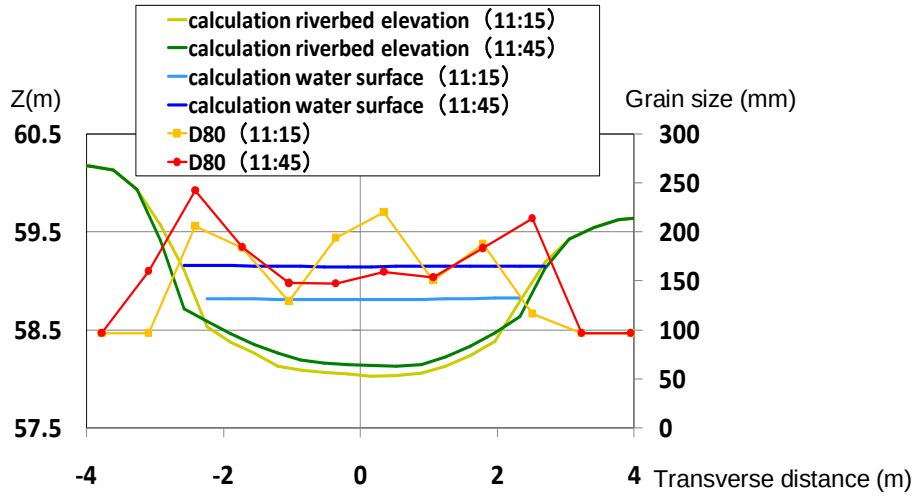

Figure 14 Calculated result of d_{80} cross-sectional distribution

4. CONCLUSIONS

We developed the two-dimensional riverbed variation analysis method focused on the mechanism of sediment transport in stony-bed rivers. This method was applied to field experiments in the Jyoganji River. As a result, it is capable of explaining water surface profile, bed variation, grain size distribution and flow discharge hydrograph in stony-bed rivers. Moreover, we showed that sediment transport rate of the cobble-class material becomes larger than the others size group. Further investigation is required to make clear the reproducibility of the riverbed scouring near the bank and channel deformation during a flood by the two-dimensional model.

REFERENCES

Fukuoka,S. (2008). Flood Flow and Bed Variation Analysis Considering the Change in Sediment Environment -Practical Issues and Perspectives of the Sediment Research-, Advance in River Engineering, JSCE, Vol.14, pp.1-6.

Fukuoka,S. and Abe,T. (2007). Mechanism of Low Water Channel Formation and the Role of Grain-Size Distribution in Gravel-bed Rivers, 10th International Symposium on River Sedimentation, Moscow, Russia.

Fukuoka,S., Osada,K. and Abe,T. (2008). The Role of Stones on The River Bed Stability in Stony Bed Rivers, Annual Journal of Hydraulic Engineering, JSCE, Vol.52, pp.643-648

Fukuoka,S. and Osada,K. (2009). Sediment Transport Mechanism and Grain Size Distributions in Stony Bed Rivers, 33rd IAHR Congress: Water Engineering for a Sustainable Environment, Vancouver, Canada, pp.505-512

Hasegawa,K. (1981). Bank-Erosion discharge based on a non-equilibrium theory, Proceedings, JSCE, No.316, pp.37-50.

Nagata,N., Hosoda,T. and Muramoto,Y. (1999). Characteristics of River Channel Processes with Bank Erosion and Development of Their Numerical Models, Journal of Hydraulic, Costal and Environmental Engineering , JSCE, Vol.621, Ⅱ-47, pp.23-39.

Osada,K. and Fukuoka,S. (2008). Development of One-dimensional Bed Variation Analysis Methods Focused on the Mechanism of Sediment Transport in Stony-Bed Rivers, Advances in Hydro-Science and Engineering, Vol.8, ICHE Nagoya, Japan.